Road surface condition sensor based on scanning detection of backward power

Songsong Xu (徐松松), Chi Ruan (阮 驰)*, and Lili Feng (冯丽丽)

State Key Laboratory of Transient Optics and Photonics, Xi'an Institute of Optics and Precision Mechanics, Chinese Academy of Science, Xi'an 710119, China

**Corresponding author: ruanchi@opt.ac.cn*

Received December 17, 2013; accepted March 27, 2014; posted online April 30, 2014

A method of detecting dry, icy and wet road surface conditions based on scanning detection of single wavelength backward power is proposed in this letter. The detector is used to receive the backward scattered power which changes with the incidence angle. The relationship between backward power and incidence angle is used to find out the effective angle range and distinguish method. Experiment and simulation show that it is feasible to classify these three conditions within incidence angle of 5.3 degree.

OCIS codes: 080.1753, 040.0040, 280.1350, 290.5880.
doi: 10.3788/COL201412.050801.

Roadway conditions are very important for traffic safety[1]. According to statistics,the probability ratio of traffic accidents that occur on icy, wet and dry surface is 4.2:1.6:1[2]. If a warning mechanism of monitoring surface weather condition is established, the management department could take effective measurements timely and drivers could be informed to lower speed especially at night. Thus, traffic accidents caused by bad weather could be effectively reduced.Usually, detection means are divided into two types:contact and non-contact methods. The contact method can effectively measure various difficult road surface conditions with high precision, while it needs construction on road surface which will reduce road service life and has the disadvantage of inconvenient construction.By contrast,the non-contact method is quite convenient, as it distinguishes surface conditions by measuring the spectral response of road surface without construction. A technique combing 1690, 1490 and 1310-nm laser diodes together is testified well in distinguishing road surface conditions[3]. However, very few laser diodes are at the wavelength 1690-nm and the cost may be very high. The solution for this method is to replace the 1690-nm laser with polarization test[4,5]. ATV-camera[6] method with image processing technique is used with the fact that the reflected light from wet surface is plane polarized, but this technique can only tell wet surface from dry condition.Another method achieves theta skin which a laser diode and a detector combine to differentiate the surface condition as water and ice absorb differently in near-infrared region[7]. However, both polarization detection and multiple wavelength technique are too systemically complicated to be an economical means. In this letter, a non-contact sensor based on single wavelength backward power and scanning detection with good economy, simple structure, high precision and convenient construction was developed.

The detection set includes a semiconductor laser, a photo-detector, a beam expander and a data acquisition device (Fig. 1). The semiconductor laser with central wavelength of 1550 nm is fiber coupledoutput.The output light irradiates on road surface through a beam expander connected to the end of the fiber to make a relatively big light spot that is about one to two hundred millimeters in length. The photo-detector with a detection span from 1000 to 1700 nm receives the reflected backward power.

When the output laser irradiates on the surface,diffuse reflection occurs as the surface is rough enough and the detector receives backward power as the incidence angle is the receiving angle. Oncewater or ice lays on the surface,the changes of surface morphology and medium will make the backward power different. Thus the dry, icy and wet road conditions are distinguished according to backward power received by the detector.

We propose an innovative detection way: scanning detection. For a determined road area, the incidence angle of laser changes while the photo-detector detects the backward scattered power at the same time. The surface

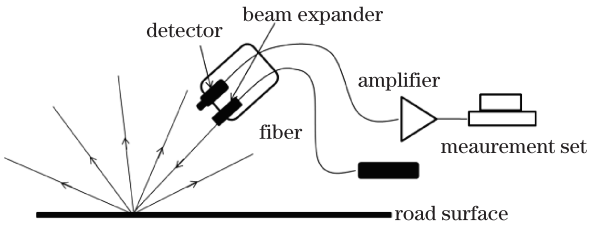

Fig. 1. Diagrammatic of the detection set.

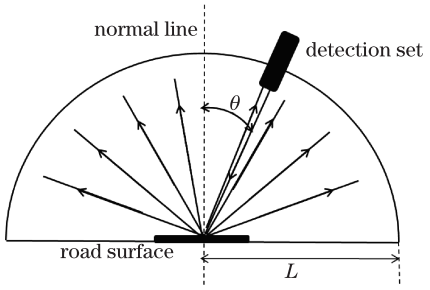

Fig. 2. Diagrammatic of experiment.

condition is judged by there lat ions hip between backward power and incidence angle. Thus, the key point is to understand the relationship between backward power and incidence angle, to establish theoretical simulation models and to find the effective incidence angle range of class ification.As shown in Fig. 2, the laser irradiates on the sample surface and the detector receives the backward power. The incidence angle is changed in 2° as a unit while the distance between the detection set and the sample surface, L, is kept constant.

The dry road surface is regarded as a diffuse reflector[8] that obeys Lambert cosine law[9,10]:

$$P(\theta) = I_0 \cos\theta \cos\theta S \Delta\Omega \tag{1}$$

Where θ is the incidence angle, I_0 is the light power density in the direction of surface normal line when θ is 0°, S is the surface area seen in the detector field of view, $\Delta\Omega$ is the solid angle subtended by the detector seen from the target[11,12]. In the experiment, S is smaller than the light spot area. As a result of the fixed field of view determined by the detector surface area, $\cos(\theta)S = S^*$, where S^* is the projection of S on a surface normal to the backward direction. So, S^* is a constant that does not vary with θ. The power received by the detector is

$$P_{\text{back}} = I_0 S^* \int\int_{\Omega} \sin\theta \cos\theta \mathrm{d}\varphi \mathrm{d}\theta = \frac{I_0 S^* r^2}{L^2} \cos\theta. \tag{2}$$

Where r is the diameter of the detector target surface; L is the distance between detector target surface and road surface.In the experiment, the power of laser output is 50 mw, r is 5 mm and L is about 3meters. In order to protect the eyes of people from strong light, a pyroelectric detector could be used to stop the laser once someone steps into the detection area.The backward power at varying incidence angleswas simulated and the results are showed in Fig. 3.

In Fig. 3, the red curve represents the theoretically simulated data and the black dots represent the experimentally measured data in a unit of 2°. The simulated data and experimental data are well consistent on the whole. P_{back} declines slowly with the increasing θ and there is still strong backward powereven when θ is close to 60°. As a result of the good consistence between simulation and experiment, it is feasible to regard the road surface as a Lambert.

When the road surface is covered by ice, the ice surface is smoother than dry condition when water freezes into

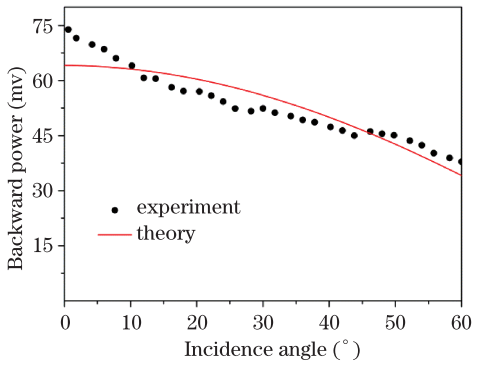

Fig. 3. Relationship between P_{back} and θ on dry condition.

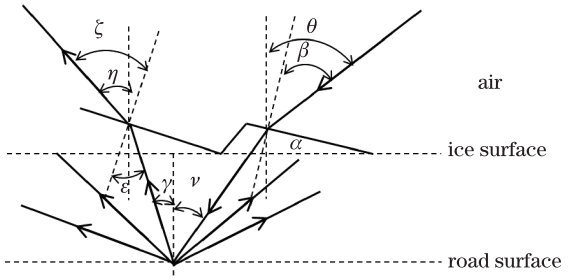

Fig. 4. Schematic diagram of icy surface.

ice as a result of water surface tension. The ice surface was modeled to be composed of countless ice planes with an angle α to the level and α was considered as a random variable to any plane with a range from $-0.5\ \pi$ to $0.5\ \pi$. Wetry to establish the following model:the proportion of α, $f(\alpha)$, obeys Normal distribution.

When the laser irradiates on the icy surface, a part of light is reflected by the surface at all directions (Fig. 4). Of the reflected light, the backward power $P_{\text{back1}}(\theta)$ is received by the detector. Another part transmitted into the ice layer is reflected by the road surface and finally refracted into the air. The backward power $P_{\text{back2}}(\theta)$ is received by the detector as well. In this letter, we only considerthese twotypes of backward power:

$$P_{\text{back}}(\theta) = P_{\text{back1}}(\theta) + P_{\text{back2}}(\theta). \tag{3}$$

The light path is showed in Fig. 4, where α is the tilt angle of ice plane, θ is the incidence angle, β is the angle between incident light and the normal line of ice plane. ν is the incidence angle of road surface under ice layer, γ is the reflectance angle of road incident light. ε is the incidence angle of ice plane. ζ is the refraction angle of ice plane, η is the angle between refraction light and the vertical normal line.

$P_{\text{back1}}(\theta)$ is just from the ice planes with α in the range of $[\theta - \frac{r}{2L}, \theta + \frac{r}{2L}]$.

$$P_{\text{back1}}(\theta) = \frac{PRr}{L} \int_{\theta-\frac{r}{2L}}^{\theta+\frac{r}{2L}} f(\alpha)\mathrm{d}\alpha, \tag{4}$$

where R is the reflectivity of ice when β is 0°. R represents the reflectivity of allthe planes withvarying angle within $[\theta - \frac{r}{2L}, \theta + \frac{r}{2L}]$ as L is larger than r.

The key point for calculation of $P_{\text{back2}}(\theta)$ is the light power distribution with angle η. When the incidence angle is θ, the angle ν, and the transmittance, $t(\alpha, \theta)$, is determined for the ice plane with the angle α. Then, the refraction light is diffusely reflected by theroad surface and the diffuse light is proportional to the cosine of ν. So,. the proportion of the diffuse light power on the laser output power is

$$X = \rho \int_{-\pi/2}^{\pi/2} f(\alpha)[t(\alpha, \theta)\cos(\nu)]\mathrm{d}\alpha, \tag{5}$$

where ρ is the reflection coefficient of road surface.The diffuse light reflected by the road surface obeys lambert cosine law in the ice layer and the probability density function of γ is $g(\gamma) = \frac{\cos\gamma}{2}$.

Obviously, $\varepsilon = \gamma - \alpha$, $\sin(\zeta) = n\sin(\varepsilon)$, $\eta = \zeta - \alpha$; n is the refractive index of ice. We get $\eta = \arcsin(n\sin(\gamma - \alpha)) - \alpha$

and $\gamma = \arcsin\frac{\sin(\eta+\alpha)}{n}$. As γ and α are two independent random variables, the joint probability density function is the product of the probability density function of the two variables. Thus, $z(\alpha, \gamma) = f(\alpha)g(\gamma)$. Then, $h(\eta)$, the probability density function of η, is calculated as

$$h(\eta) = \int_{-\pi/2}^{\pi/2} z(\alpha,\gamma)\left|\frac{\mathrm{d}\gamma}{\mathrm{d}\eta}\right|\mathrm{d}\alpha = \int_{-\pi/2}^{\pi/2} z\left(\alpha, \arcsin\frac{\sin(\eta+\alpha)}{n}+\alpha\right)\left|\frac{\mathrm{d}\gamma}{\mathrm{d}\eta}\right|\mathrm{d}\alpha. \quad (6)$$

The light transmitted into air is relative to the transmittance of each ice plane, so the transmittance of $\eta, T(\eta)$, need to be calculated. For the incident light which has thesame η, it is known that the angle γ is determined by α. For the incident light whose refraction light is with the same angle η, the probability density function is

$$k_\eta(\alpha) = \frac{f(\alpha)g(\gamma)}{\int_{-\pi/2}^{\pi/2} f(\alpha)g(\gamma)\mathrm{d}\alpha} = \frac{f(\alpha)g(\alpha,\eta)}{\int_{-\pi/2}^{\pi/2} f(\alpha)g(\alpha,\eta)\mathrm{d}\alpha}. \quad (7)$$

Thus,

$$T(\eta) = \int_{-\pi/2}^{\pi/2} k_\eta(\alpha)\mathrm{d}\alpha = \int_{-\pi/2}^{\pi/2} \frac{f(\alpha)g(\alpha,\eta)t(\alpha,\eta)}{\int_{-\pi/2}^{\pi/2} f(\alpha)g(\alpha,\eta)\mathrm{d}\alpha}\mathrm{d}\alpha = \frac{\int_{-\pi/2}^{\pi/2} f(\alpha)g(\alpha,\eta)t(\alpha,\eta)\mathrm{d}\alpha}{\int_{-\pi/2}^{\pi/2} f(\alpha)g(\alpha,\eta)\mathrm{d}\alpha}, \quad (8)$$

where $t(\alpha,\eta)$ is the transmittance of ice plane. So the light distribution function is $h(\eta)T(\eta)$. Thus, the backward power received by the detector is

$$P_{\mathrm{back2}}(\theta) = \frac{PXr}{L}\int_{\theta-\frac{r}{2L}}^{\theta+\frac{r}{2L}} H(\eta)T(\eta)\mathrm{d}\eta, \quad (9)$$

$$P_{\mathrm{back}}(\theta) = P_{\mathrm{back1}}(\theta) + P_{\mathrm{back2}}(\theta) = \frac{PRr}{L}\int_{\theta-\frac{r}{2L}}^{\theta+\frac{r}{2L}} f(\alpha)\mathrm{d}\alpha + \frac{PRr}{L}\int_{\theta-\frac{r}{2L}}^{\theta+\frac{r}{2L}} h(\eta)T(\eta)\mathrm{d}\eta. \quad (10)$$

Figure 5 shows the theoretical simulation curve and experimentally measured data, which are in good consistence on the whole. When θ is 0°, P_{back} is maximized to be 300 mv. After that, $P_{\mathrm{back}}(\theta)$ declines quickly with the increase of θ until 6°, where $P_{\mathrm{back}}(\theta)$ is largely different from dry condition: $P_{\mathrm{back}}(\theta)$ of icy condition is larger at small angle and smaller atlarger angle than dry condition.

Like the icy surface,the surface covered by water was modeled to be composed of planes with angle κ,the proportion of which obeys Normal distribution, to the level.Thus,the calculation of backward power is similar to that on the icy surface.However, the standard deviation in Normal distribution of water surface is smaller than that of icy surface as the surface tension of water greatly diminishes the roughness of the road surface. The relationship between P_{back} and θ is showed in Fig. 6.

In Fig. 6,the red curve represents theroretically simulated data and the black dots represent experimental measurements. On the whole, they fit well with negligible error at large incidence angle. P_{back} declines more rapidly with the increase of θ within 6° than icy condition. At 0°, P_{back} is maximized to be 350 mv, which is slightly higher than that on the icy condition.

The theroretically simulated data of dry,icy and wet surfaces are showed in Fig. 7 for comparision. The value of P_{back} on icy and wet conditions are so close at large incidence angle that the two conditions can be hardly distinguished at more than 5.3°.

There are relatively big differences among three conditions within 5.3°, and thus further study is needed to search an appropriate classification method. Figure 8 shows three intersectiones among the three curves from 0° to 5.3°: 0.9°, 1.8°, 3.4°. Thus four sectiones are devided:

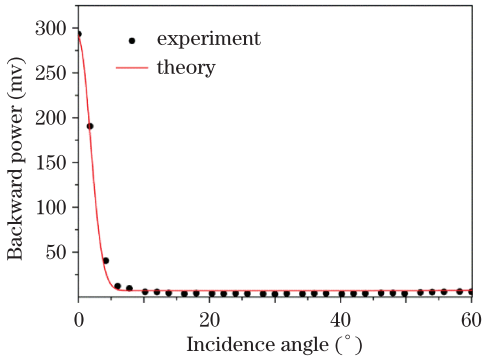

Fig. 5. Relationship between P_{back} and θ on icy condition.

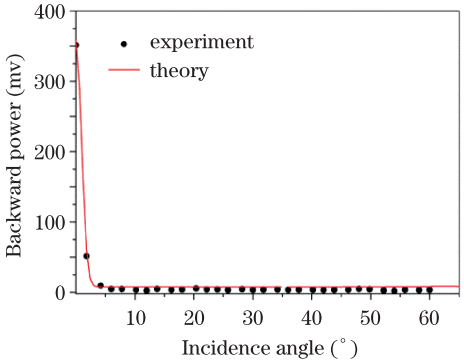

Fig. 6. Relationship between P_{back} and θ of wet surface.

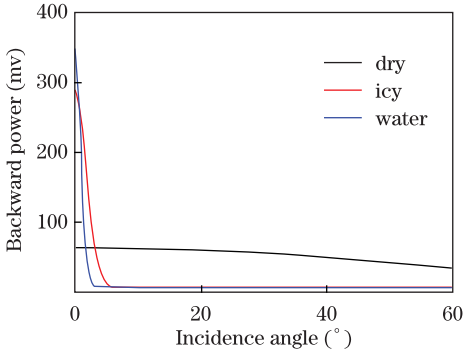

Fig. 7. Relationship between P_{back} and θ on dry, icy and wet surface.

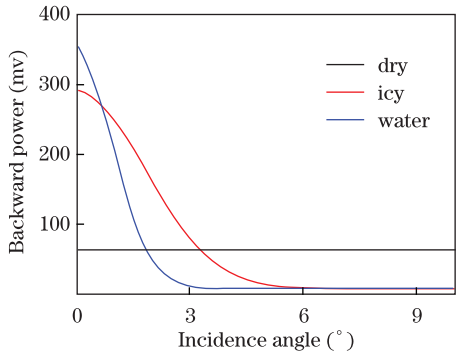

Fig. 8. Relationship between P_{back} and θ on dry, icy and wet surface within 10°.

$$1.\ 0.9^\circ > \theta > 0^\circ, \quad P_{\text{back}}(\text{water}) > P_{\text{back}}(\text{icy}) > P_{\text{back}}(\text{dry}); \tag{11}$$

$$2.\ 1.8^\circ > \theta > 0.9^\circ, \quad P_{\text{back}}(\text{icy}) > P_{\text{back}}(\text{water}) > P_{\text{back}}(\text{dry}); \tag{12}$$

$$3.\ 3.4^\circ > \theta > 1.8^\circ, \quad P_{\text{back}}(\text{icy}) > P_{\text{back}}(\text{dry}) > P_{\text{back}}(\text{water}); \tag{13}$$

$$4.\ 5.3^\circ > \theta > 3.4^\circ, \quad P_{\text{back}}(\text{dry}) > P_{\text{back}}(\text{icy}) > P_{\text{back}}(\text{water}). \tag{14}$$

The relationship among Eqs. (11), (12), (13), and (14) can be used to classify three conditions and scanning detection can definitely improve the detection precision.

In conclusion, we develop a non-contact road surface weather condition sensor based on single wavelength backward power and scanning detection with the advantage of good economy, simple strcture, high precision and easy installation. We study the relationship between backward power and incidence angle under different surface conditions and establish the modles of dry, icy and wet surfaces for theroretical simulation, which fits well with experimentally measured data. The effective incidence angle range is found out and it is feasible to distinguish three conditions within 5.3°. However, it is difficult to distinguish the snowy surface with a single wavelength light source. The geometrical optics theory in the paper does not apply to the snowy condition as the reflectivity of snow is greatly relevant to wavelength in near-infrared. We study and experimently measure the spectrum characteristics of snow. It is found that the useful wavelength is 1064 and 1550 nm: at 1064 nm, the reflectivity of snow is close to that of dry surface, while at 1550 nm, the reflectivity of snow is far more less than that of dry surface. Thus, the snowy condition could be identified.

References

1. C.-G. Wallman and H. åström, VTI meddelande 911A(2001).
2. T. Yan, Z. Zhiqiang, Z. Jinghan, Z. Yulan, Meterological, Hydrological and Marine Instrument **2,** 87 (2011).
3. J. Casselgren, M. Sjödahl, and J. LeBlanc, Appl. Opt. **46,** 4277 (2007).
4. J. Casselgren and M. Sjödahl, Appl. Opt. **46,** 3036 (2012).
5. F. S. Harris, Jr., Appl. Opt. **10,** 732 (1971).
6. M. Yamada, T. Oshima, K. Ueda, I. Horiba, and S. Yamamoto, JSAE Rev. **24,** 183 (2003).
7. F. Holzwarth and U. Eichhorn, Sens. Actuators **37,** 121 (1993).
8. K. Jiang, K. Yu, and Y. Zhao, Chin. Opt. Lett. **10,** 042101 (2012).
9. K. C. Jezek and G. Koh, Appl. Opt. **26**, 5143 (1987).
10. A. Gross, Appl. Opt. **22,** 3031 (1983).
11. D. C. Look, Jr. J. Opt. Soc. Am. **55,** 1628 (1965).
12. G. Xu, Y. Pang, and Z. Li, Chin. Opt. Lett. **11,** 082801 (2013).